THE UNIVERSITY OF ZAMBIA

SCHOOL OF ENGINEERING

Department of Electrical and Electronic Engineering

Energy Systems and Electrical Machines Division

INDUCTION MACHINE MODELS

BY

YUMBA BONIFACE

November 2005

ACKNOWLEDGEMENTS

I pay my thanks of gratitude to the almighty God who has made this report a reality.

The material in this report has been prepared with valuable assistance of the following, to whom am greatly indebted.

I further thank my project supervisor, Mr. A.A. Zulu, for the time spent making very constructive suggestions and comments, especially for his keen interest to see the project succeed.

I also wish to express my gratitude to the technical staff at the Electrical Machines Laboratory; in particular Mr. A. Banda and Mr. T. Gondwe for providing the necessary equipment relating to the project.

DEDICATIONS

I would like to dedicate this report to my family and friends. Thank you for the support rendered.

TABLE OF CONTENTS

CHAPTER ONE

CHAPTER TWO

2.0 EXPERIMNTAL RESULTS AND DATA ANALYSIS

CHAPTER THREE

3.0 DYNAMIC MODELING OF INDUCTION MACHINES

CHAPTER FOUR

4.0 DISCUSSIONS AND CONCLUSION

APPENDICES

LIST OF TABLES AND FIGURES

Figures

Tables

NOTATION

f_s	Utility supply frequency or stator supply frequency, Hz
i_{abc}	*abc* phase current vector
i_{as}, i_{bs}, i_{cs}	Instantaneous *a*, *b* and *c* stator phase currents, A
I_c	Core-loss current per phase, A
i_{ds}, i_{qs}	*q* and *d* stator currents, A
I_m	Magnetising current per phase, A
i_{qdo}	*qdo* current vector
I_{rms}	RMS rotor current referred to the stator, A
I_s	RMS stator- phase current, A
I_{sc}	RMS stator- phase current when rotor is locked, A
L_{lr}	Stator-referred rotor-leakage inductance per phase, H
L_{ls}	Stator-leakage inductance per phase, H
L_m	Magnetising inductance per phase, H
L_r	Stator-referred rotor self-inductance per phase, H
L_s	Stator self-inductance per phase, H
n_r	Rotor speed, rpm
n_s	Synchronous speed, rpm
p	Differential operator
P	Number of poles
P_{oc}	Core-loss, W
P_{sc}	per-phase copper losses, W
R_c	core-lose resistance, Ω
R_r	Stator-referred rotor-phase resistance, Ω
R_s	Stator resistance per phase, Ω
T1	number of turns in phase
T_{abc}	Transformation from *abc* to *qdo* axes
v_{abc}	*abc* voltage vector
V_{as}, V_{bs}, V_{cs}	RMS stator phase *a*, *b* and *c* voltages, V
V_{sc}	RMS stator- phase voltage applied when rotor is locked, V
X_{eq}	Total leakage reactance per phase, Ω
X_{lr}	Stator-referred rotor-leakage reactance per phase, Ω

X_{ls}	Stator-leakage reactance per phase, Ω
Z_{eq}	Equivalent impedance, Ω
Z_{sc}	Stator-phase short-circuit impedance, Ω
θ_c	Arbitrary lag angle between *q* axis and a phase windings, rad
θ_r	Rotor position with respect to d axis, rads
θ_s	stator –current phasor angle, rad
θ_{sl}	slip angle, rad
ω_r	Electrical rotor speed, rad/sec
ω_s	Supply angular velocity, rad/sec
ω_{sl}	Slip speed or slip angular frequency, rad/sec

PROJECT SUMMARY

The objectives of this project were to study different induction machine models in classical and modern control, and predicting performance with parameters of a representative laboratory machine using Matlab® and Simulink™.

The dynamic model of the three-phase induction motor was derived by using a two-phase motor in direct and quadrature axes. The equivalence between the three-phase and the two-phase models was derived from simple observation. The equivalence is based on the equality of the magnetomotive force (mmf) produced in the two-phase and there-phase windings and equal current magnitude. The required transformation in voltages and currents was derived in a generalized way. Reference frames were chosen to be arbitrary, and three particular cases of the generalized model of the induction motor in arbitrary reference frames considered were: stator, rotor and synchronously rotating reference frames models.

The induction motor simulation models were developed by using the differential equation models (state-variable models). Simulation models of stator phase current, magnetising current and q- and d-axis rotor current response in stator reference frames were considered.

CHAPTER ONE

1.0 INTRODUCTION

The induction motor, which is the most widely used motor type in the industry, is favored because of its good self-starting capability, simple and rugged structure, low cost and high reliability.

During the recent years, the significance of the squirrel-cage induction motors in speed and position controlled drives has grown drastically. The reason is the large-scale exploitation of the a.c induction motors in the technologies, which traditionally used d.c motors. Furthermore, to achieve high efficiency of the technology, many non-controlled a.c drives are reconstructed by adding frequency converters and they are used now as speed controlled drives. To attach perfect static and dynamic qualities of these drives, control engineers need more information about the control object. Therefore, the importance of the models, characteristics and parameter determination of squirrel-cage induction motor has markedly grown. The most important means of the drive design and control is an advanced model of a motor. Moreover, the model-based control methods of the induction motor drives are most effective and usable.

In the present context, a model is a formulation of part or of the whole of the machine system in terms of the appropriate parameters and on the basis of some acceptable theory of behavior. The aim is to observe the response of the model to a given stimulus, so that its behavior can then be translated into the comparable performance of the prototype.
The model must have the appropriate parameters, and enough of them to give useful results. The choice of parameters is dictated by the stimulus to be applied and the response expected; and there must be some theory of behavior into which the parameters will fit.

Many different models available for squirrel-cage induction motors are successfully used for drive design and control. Generally, these models can be classified as static or dynamic, single or multi-phase, linear or non-linear as illustrated in figure 1.1. In addition, models with lumped or distributed parameters also exist.

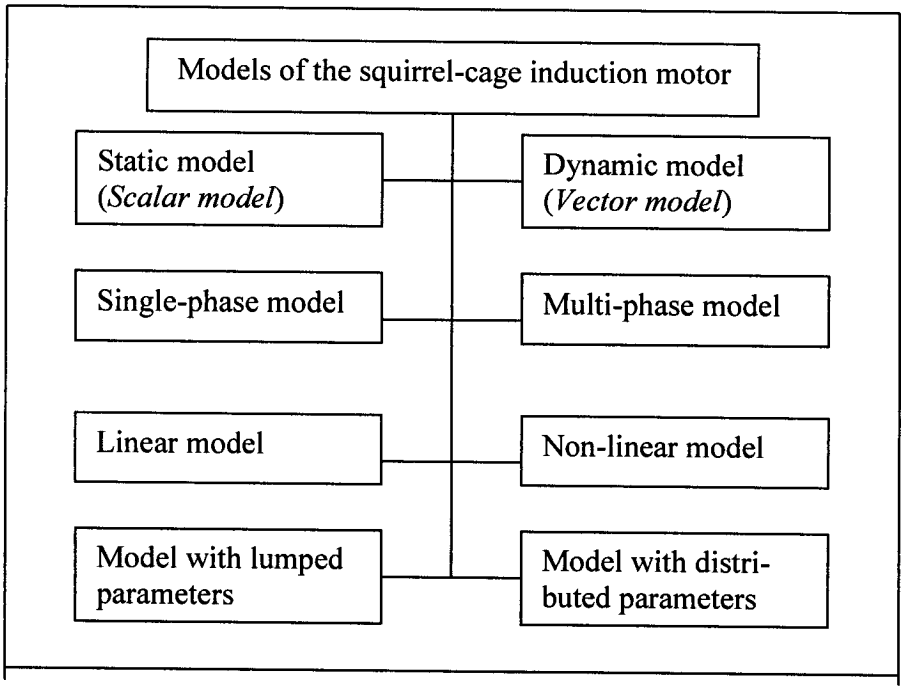

Figure 1.1: The classification of models

1.1 Background

Although almost all applications of induction machines invariably require operation in the steady state, number of applications or situations may occur which place emphasis on dynamic (or transient) performance. Analysis viewpoint show that both the steady state and dynamic performance characteristics are theoretically available from differential equations of motion. These equations are readily obtainable with help of equivalent circuit model and matrix equations that may either be linear or non-linear. Some non-linear equations cannot be linearised and solved analytically upon making approximations. Thus development of models become necessary and lead to computer simulations that indicate the machine performance.

The principle of operation of the induction motor is developed to derive the steady state equivalent circuit and performance calculations. These are required to evaluate the steady state response of variable-speed induction motor drives. The dynamic simulation is one of the key steps in the validation of the design process of motor-drives, eliminating inadvertent

design mistakes and the resulting errors in the prototype construction and testing, and hence the need for dynamic models of the induction machine.

1.2 Problem Statement.

One way of investigating the performance of an induction motor is by use of the equivalent circuits. While the performance of an induction motor can be done in this way, there are benefits and limitations.

1.3 Rationale

Various models of induction machines will be investigated from simple to most detailed ones in order to carry out an increasingly detailed analysis of the machine.The choice of the model will strongly depend on the machine purpose and the computational tools available for satisfactory performance prediction.

1.4 Study Objectives

The project aims its focus on:

1. The study of different induction machine models in classical and modern control.
2. Predicting performance with parameters of a representative laboratory machine using Matlab® and its toolbox Simulink™.

1.5 Literature Review

A single-phase equivalent circuit with lumped parameters is the mostly used traditional model in analysis and design of an AC induction motor. In the "per-phase equivalent circuit," it is noted that all the rotor parameters and variables are not actual quantities but are quantities referred to the stator. Methods of determining circuit parameters from no-load test and locked-rotor test are described in chapter two. It is also known that induction motors do not rotate synchronously to the excitation frequency. At rated-load, the speeds of induction motors are slightly (about 2-7 % in many cases) less than the synchronous speed. If the synchronous speed is n_s, and the actual rotor speed n, then slip s, is defined by:

$$s = (n_s - n)/n_s$$

Note that slip is non-dimensional and is one of the most important variables in the control and operation of the induction machines.

There are many kinds of equivalent circuits used to calculate the static speed-torque characteristics as illustrated in figure 1.2. The equivalent circuits **a** and **b** could be successfully used for wound rotor induction motors. The scheme **c** could be used for induction motors with large air-gap, such as magnetohydrodynamical (MHD) pumps and some types of linear motors. Because of the large air-gaps of these machines, the mutual inductance between primary and secondary windings is small and secondary effects can be considered in the series circuit of the resistance and inductance. The rotor resistance R_r' and rotor inductance L_r' are complex functions of slip, conductivity and boundary effects of the secondary system. In special cases, also the scheme **d** or **e** could be used. The scheme **e** is useful for the analysis of vector controlled a.c induction motor drives, where the electromotive force is observed and the a.c motor like a d.c motor can be accepted.

In many cases, the core-loss resistance R_c, is neglected as its large value acts like an open circuit for the current through its branch.

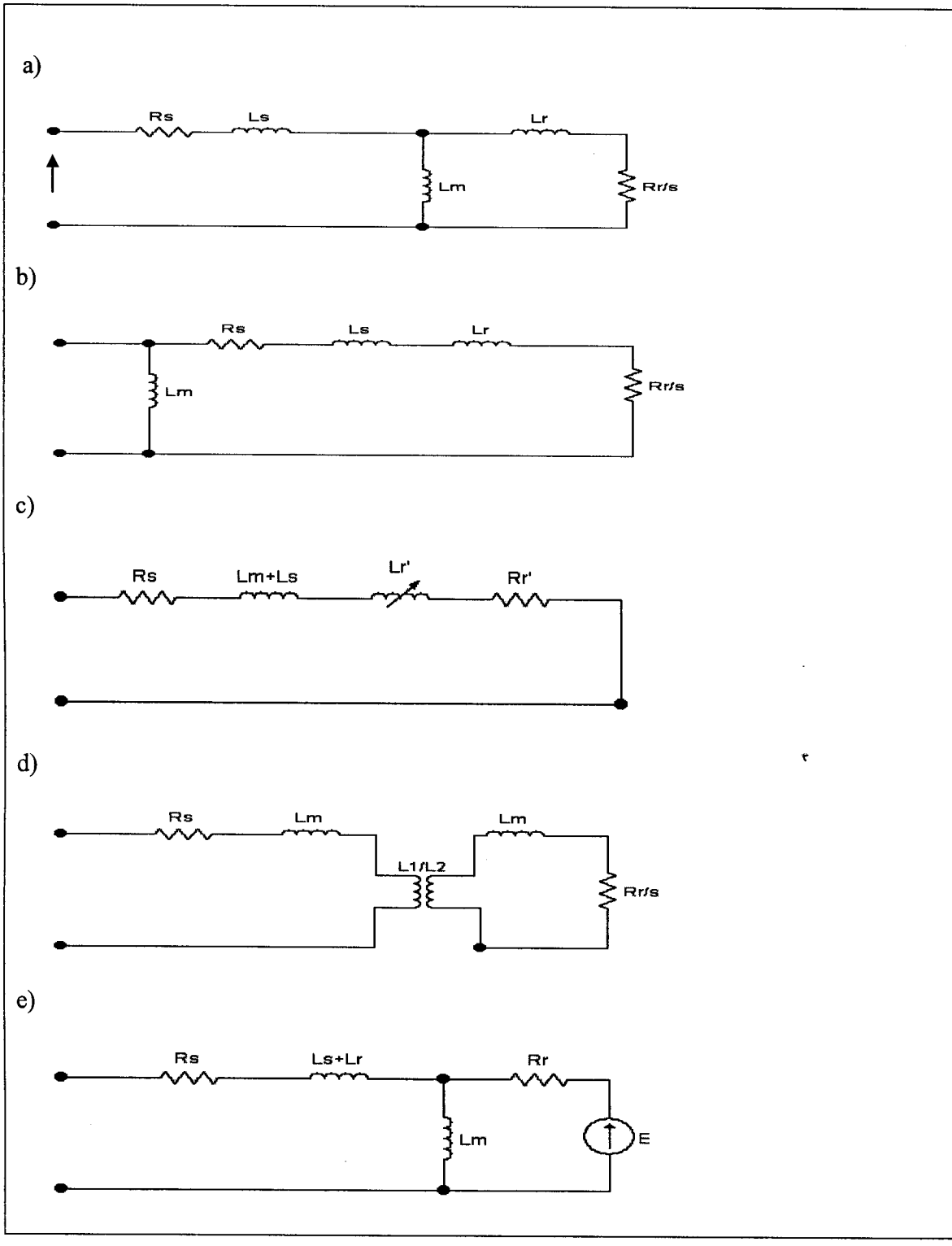

Figure 1.2: The Equivalent Circuits of Induction motor

The standard *qd* induction motor model has been recognized for some time in literature. Although it is capable of estimating the fundamental component of the current and the average value of torque near rated operating conditions, the accuracy deteriorates at other operating points. Of particular concern in drive design is the fact that it underestimates the amount of current and torque ripples by a factor of two or five. A commonly employed alternative to a lumped-parameter *qd*- model is finite element analysis (FEA), which is widely used in the design of induction machines but to a lesser extent for drive analysis due to its increased computational burden. The *qd*-model is well suited to drive analysis since it is readily linked to power converter, switching level (modulation) control, supervisory control, and mechanical system models. Simulation using this class of model executes very rapidly in comparison with time domain FEA models.

The steady-state model and equivalent circuit are useful for studying the performance of the machine in steady state. The performance features normally of interest are the voltage, current, power and torque. The instantaneous effects of varying voltages or currents, stator frequency are considered in dynamic models. The dynamic model of the induction machine in direct-, quadrature-, and zero-sequence axes (known as *dqo* or *dq* axes) is derived from fundamentals. This is generally considered difficult and hence care is taken to maintain simplicity in the derivation, while physical insight is introduced. The *dqo* model uses two windings for each of the stator and rotor of the induction machine. The transformations used in the derivation of various dynamic models are based on simple trigonometric relationships obtained as projections on a set of axes. The dynamic model is derived with the frames of observation rotating at an arbitrary speed. The most useful models in stationary, rotor and synchronous reference frames are obtained as particular cases of the arbitrary reference frames. The dynamic model is used to obtain transient responses, small-signal equations and a multitude of transfer functions, all of which are useful in the study of converter-fed induction motor drives. Space-phasor approach has further simplified the polyphase induction machine models to one equivalent stator and one rotor winding, thereby evoking a powerful similarity to the d.c machine to correspond with its armature and field windings.

CHAPTER TWO

2.0 EXPERIMENTAL RESULTS AND DATA ANALYSIS

2.1 Measurements on Experimental Machine

The objective of this experiment was to determine the squirrel-cage induction motor per-phase equivalent circuit parameters. These results of the experiment were used in the detailed analysis of the machine.

2.1.1 **Introduction**

The induction motor is basically a transformer, whose secondary rotates with respect to the primary. The stator windings produce flux that crosses the air-gap and cuts the rotor conductors.

The operating characteristics may be determined by performing three tests. These are (1) the *no-load* test, (2) the *load* test, and (3) the *stator-resistance* test. Power is applied to the motor operating free, i.e. without load, and measurements are taken of the power input, current and voltage. The load test is performed upon the motor with load applied [1]. The third test is a simple d.c resistance measurement of the stator windings per phase. It is customary to measure the resistance between three pairs of stator terminals; the average of these values divided by 2 to obtain the resistance per phase. Since the effective a.c resistance is higher than the d.c resistance, the latter is usually multiplied by a factor of about 1.25 to obtain the former [2]. The values of the rotor resistance and the rotor reactance can be determined by performing the so-called *Locked-rotor* test. Great care should be taken when doing this because the motor temperature will rise very rapidly unless the current is not too high and instruments readings are taken quickly.

2.1.2 **Item being tested**

ETL 174 Three phase squirrel-cage induction motor

Voltage: 240V (star) / 120V (delta)

Current: 1.75 A

Poles: 2

Frequency: 50 Hz

RMP: 2880

2.1.2 **Equipment**

ETL 174N Swinging field dynamometer

Power: 500 W

Speed: 5000 rpm

Torque: ±5 Nm

1x variable single-phase power supply, 0-270 V, 50 Hz a.c

1x variable three-phase power supply, 0-270 V, 50 Hz a.c

1x 20 Ω, 400 W resistor

1x fixed d.c supply, 220 V, 1 A

1x 1A ammeter

1x 5A ammeter

1x 5A, 300 W wattmeter

2.1.4 **Circuit Diagram**

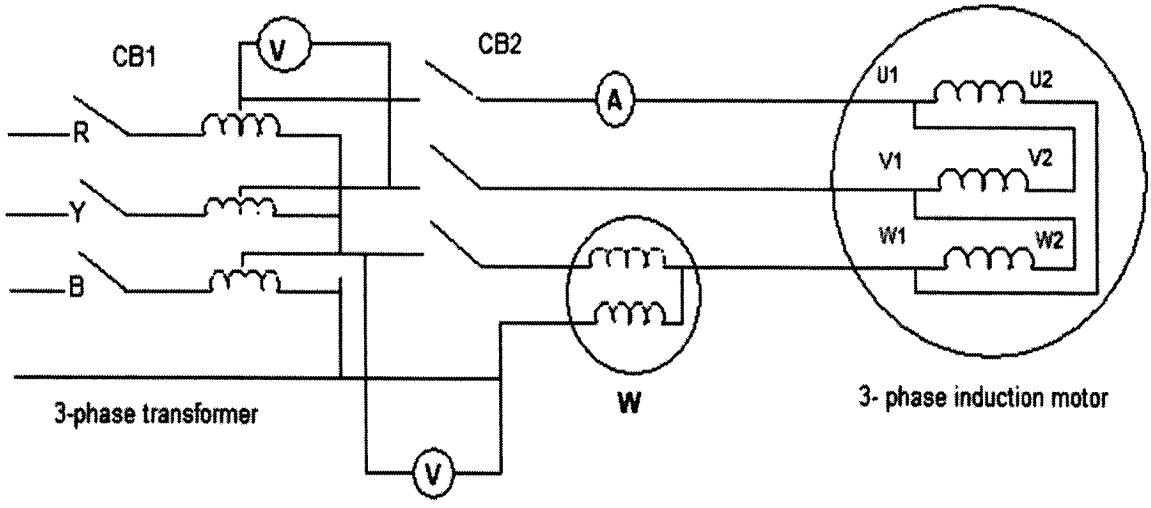

Figure 2.1: Connection diagram of three-phase motor

2.1.5 **Procedure**

2.1.5.1 The motor was connected to the three-phase variable transformer as shown fig.2.1 making sure that the circuit breakers CB2 and CB2 were in off position.

2.1.5.2 Connections to the ETL 174 Swinging Field Dynamometer were made, making sure that the ON/OFF switch was off and the variable ac supply voltage was zero.

2.1.5.3 Circuit breaker CB1 was then closed. The supply voltage of the three phase variable transformer was raised to motor rated voltage.

2.1.5.4 The supply to the ETL 174N Swinging dynamometer was switched on. The Torque/Speed Display ETL 174P LCD's would be lit.

2.1.5.5 The speed input selector switch was set to **Dynamometer**, the Speed Display selector to **Normal** and the Torque units switch to **Nm**.

2.1.5.6 **No-Load test**

Circuit breaker CB2 was closed. The motor would start running. Once it had stabilized, for the motor, the following readings were taken down: line voltage, phase voltage, no-load current, no-load power, no-load torque and no-load speed.

2.1.5.7 **Locked-rotor test**

The three-phase supply was reduced to zero and the direction of rotation of the motor was noted as it decelerated to stand- still. Having noted the direction of rotation of the rotor, the rotor was locked by means of a wedge placed in the coupling such that the rotor would not rotate in the observed direction. The three-phase supply of the variable transformer was slowly raised whilst the load current was observed until the rated value was obtained. For the motor, the following readings were taken: the line voltage, phase voltage, load current and the power.

2.1.5.8 **Starter Resistance**

The load was reduced to zero by reducing the variable field supply to zero. The three-phase supply was also reduced to zero. The circuit breakers CB1 and CB2 were opened. The resistance readings of the motor stator windings were quickly taken: U1 and U2, V1 and V2, W1 and W2.

2.1.6 Measurement Results

Table 2.1 No-Load Test

Line Voltage,V_L	Phase Voltage,V_P	No-load current,I_{NL}	No-load power, P_{NL}	Speed (rpm)	Torque (Nm)
240.8 V	141.3 V	0.47 A	35 W	2950	0.06

Table 2.2 Locked-Rotor Test

Line Voltage,V_L	Phase Voltage,V_P	Load Current,I_L	Power
79.76 V	47.00 V	1.75 A	62.50 W

Table 2.3 Starter Resistances

U1 and U2	V1 and V2	W1 and W2
10.13 Ω	10.14 Ω	10.14 Ω

2.1.7 **Calculations and Analysis**

From the stator resistance test [2],

Average d.c resistance= 10.14 Ω

Therefore, the a.c resistance of stator per phase, R_s was:

$$R_s = \frac{10.14}{2} \times 1.25 \qquad (2.1)$$

$$= \underline{6.34}\ \Omega$$

The mutual inductance and the core-loss resistance were calculated from Open circuit test as follows:

The no-load power factor is given by

$$\cos Q_{oc} = \frac{P_{oc}}{V_s I_s} \qquad (2.2)$$

$$= \frac{35}{141.3 \times 0.47}$$

$$= \underline{0.53}$$

From which the magnetizing current was calculated as

$$I_m = I_s Sin Q_{oc}$$
$$= 0.47 \times 0.85 \qquad (2.3)$$
$$= 0.4\ A$$

and the core-loss current is given by

$$I_c = I_s Cos Q_{oc}$$
$$= 0.47 \times 0.53 \qquad (2.4)$$
$$= 0.25\ A$$

The magnetizing inductance was computed from

$$L_m = \frac{V_s}{2\pi f_s \mathrm{Im}} = 1.124\ H \tag{2.5}$$

and the core-resistance is given by

$$R_c = \frac{V_s}{I_c} = 565.2\ \Omega \tag{2.6}$$

From the locked-rotor test, the parameters were calculated as follows:

The short-circuit power factor obtained from equivalent circuit is

$$Cos\ Q_{sc} = \frac{P_{sc}}{V_{sc}I_{sc}} = 0.76 \tag{2.7}$$

and the short-circuit impedance is given by

$$Z_{sc} = \frac{V_{sc}}{I_{sc}} = 26.86\ \Omega \tag{2.8}$$

from which the rotor resistance and total leakage reactance were computed as

$$R_r = Z_{sc}\cos Q_{sc} - R_s = 26.86 \times 0.76 - 6.34 = 14.07\ \Omega \tag{2.9}$$

and

$$X_{eq} = Z_{sc}\sin Q_{sc} = 17.46\ \Omega \tag{2.10}$$

where the total leakage reactance per phase, X_{eq}, is the sum of the stator and referred-rotor leakage reactances. It is usual to assume that the stator and rotor leakage reactance equal. Thus

$$X_{ls} = X_{lr} = \frac{17.46}{2} = 8.73\ \Omega \tag{2.11}$$

and the leakage inductances were

$$L_{ls} = L_{lr} = \frac{X_{ls}}{2\pi f_s} = 28\ mH \tag{2.12}$$

The stator and stator-referred rotor self-inductances are given by

$$L_s = L_m + L_{ls}$$

$$L_r = L_m + L_{lr}$$

Therefore, $L_s, L_r = \underline{1.152\ H}$ (2.13)

CHAPTER THREE

3.0 DYNAMIC MODELING OF INDUCTION MACHINES

3.1 Three-Phase to Two-Phase transformation

A dynamic model of the three-phase induction machine can be derived from the two-phase machine if the equivalence between the three and two phases is established. The equivalence is based on the equality of the mmf produced in the three-phase and two-phase windings and equal current magnitudes. Figure 3.1 shows the three-phase and two-phase windings. Assuming that each of the three-phase winding has T_1 turns per phase and equal current magnitudes, two-phase winding will have $3T_1/2$ turns per phase for mmf equality. The *d* and *q* axes mmfs are found by resolving the mmfs of the three phases along the d and q axes.

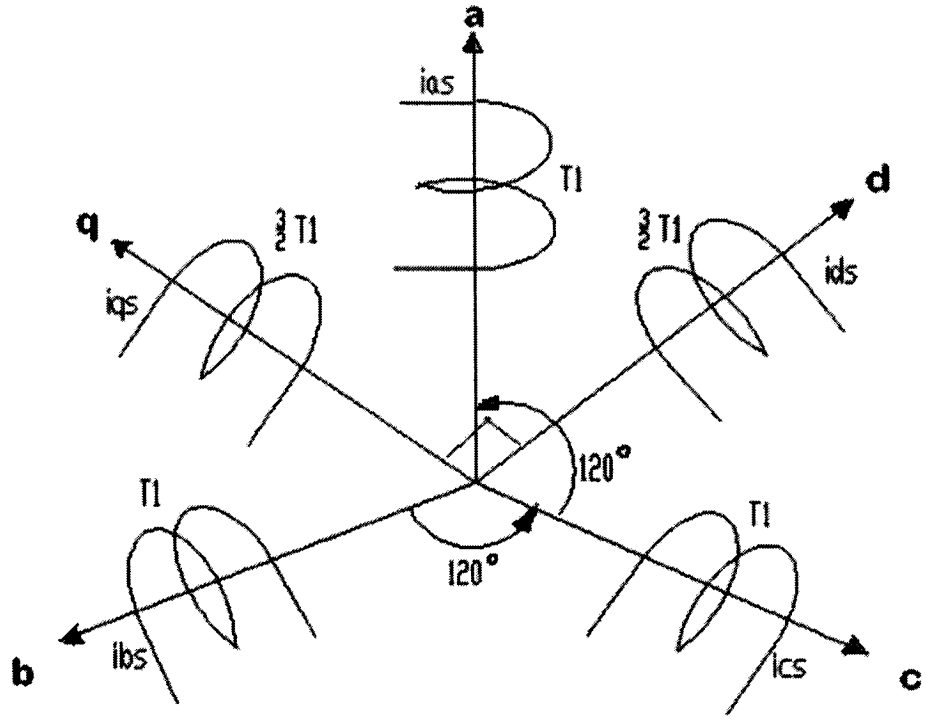

Figure 3.1: Two- and three-phase stator windings.

The common, the number of turns in the winding, is canceled on either side of the equations, leaving the current equalities. The *q* axis is assumed to be lagging the *a* axis by θ_c . The relationship between *dqo* and *abc* currents is as follows:

$$\begin{bmatrix} i_{qs} \\ i_{ds} \\ i_o \end{bmatrix} = \frac{2}{3} \begin{bmatrix} \cos\theta_c & \cos(\theta_c - \frac{2\pi}{3}) & \cos(\theta_c + \frac{2\pi}{3}) \\ \sin\theta_c & \sin(\theta_c - \frac{2\pi}{3}) & \sin(\theta_c + \frac{2\pi}{3}) \\ \frac{1}{2} & \frac{1}{2} & \frac{1}{2} \end{bmatrix} \begin{bmatrix} i_{as} \\ i_{bs} \\ i_{cs} \end{bmatrix} \tag{3.1}$$

The current i_o represent the imbalance in the a, b and c phase currents and can be recognized as the zero-sequence component of the current. Equation (3.1) can be expressed in compact form by

$$i_{dqo} = [T_{abc}]\, i_{abc} \tag{3.2}$$

where

$$i_{dqo} = [i_{qs} \quad i_{ds} \quad i_o]' \tag{3.3}$$

$$i_{abc} = [i_{as} \quad i_{bs} \quad i_{cs}]' \tag{3.4}$$

and the transformation from abc to dqo variables is

$$[T_{abc}] = \frac{2}{3} \begin{bmatrix} \cos\theta_c & \cos(\theta_c - \frac{2\pi}{3}) & \cos(\theta_c + \frac{2\pi}{3}) \\ \sin\theta_c & \sin(\theta_c - \frac{2\pi}{3}) & \sin(\theta_c + \frac{2\pi}{3}) \\ \frac{1}{2} & \frac{1}{2} & \frac{1}{2} \end{bmatrix} \tag{3.5}$$

The zero-sequence current i_o, does not produce a resultant magnetic field. The transformation from two-phase to three- phase currents can be obtained as

$$i_{abc} = [T_{abc}]\text{^}-1 \; i_{dqo} \tag{3.6}$$

where

$$[T_{abc}]\text{^}-1 = \begin{bmatrix} \cos\theta_c & \cos\theta_c & 1 \\ \cos(\theta_c - \frac{2\pi}{3}) & \sin(\theta_c - \frac{2\pi}{3}) & 1 \\ \cos(\theta_c + \frac{2\pi}{3}) & \sin(\theta_c + \frac{2\pi}{3}) & 1 \end{bmatrix} \tag{3.7}$$

3.2 Generalized Model in Arbitrary Reference Frames

Reference frames are very much like observer platforms, in that each of the platforms gives a unique view of the system at hand as well as a dramatic simplification of the system equations. For the purposes of control, it is desirable to have the system variables as dc quantities, although the actual variables are sinusoidal. This could be accomplished by having reference frames revolving at the same angular speed as that of a sinusoidal variable. As the reference frames are moving at an angular speed equal to the angular frequency of the sinusoidal supply, say, then the differential speed between them is reduced to zero, resulting in the sinusoid being perceived as a dc signal from the reference frames. Instead of deriving the transformations for each and every particular reference frame, it is advantageous to derive the general transformation for an arbitrary rotating reference frame. Then any particular reference frame can be derived by substituting the appropriate frame speed and position in the generalized reference model.

Reference frames rotating at an arbitrary speed are hereafter called arbitrary reference frames. The relationship between the stationary reference frames denoted by d and q axes and the arbitrary reference frames denoted by d_c and q_c axes are shown in figure 3.2. Assuming that the three-phase machine has balanced windings and balanced inputs, thus making the zero-sequence component be zero and eliminating the zero-sequence equations from further considerations. Note that the zero-sequence equations have to be included only for unbalanced operation of the motor, a situation common with a fault in the machine.

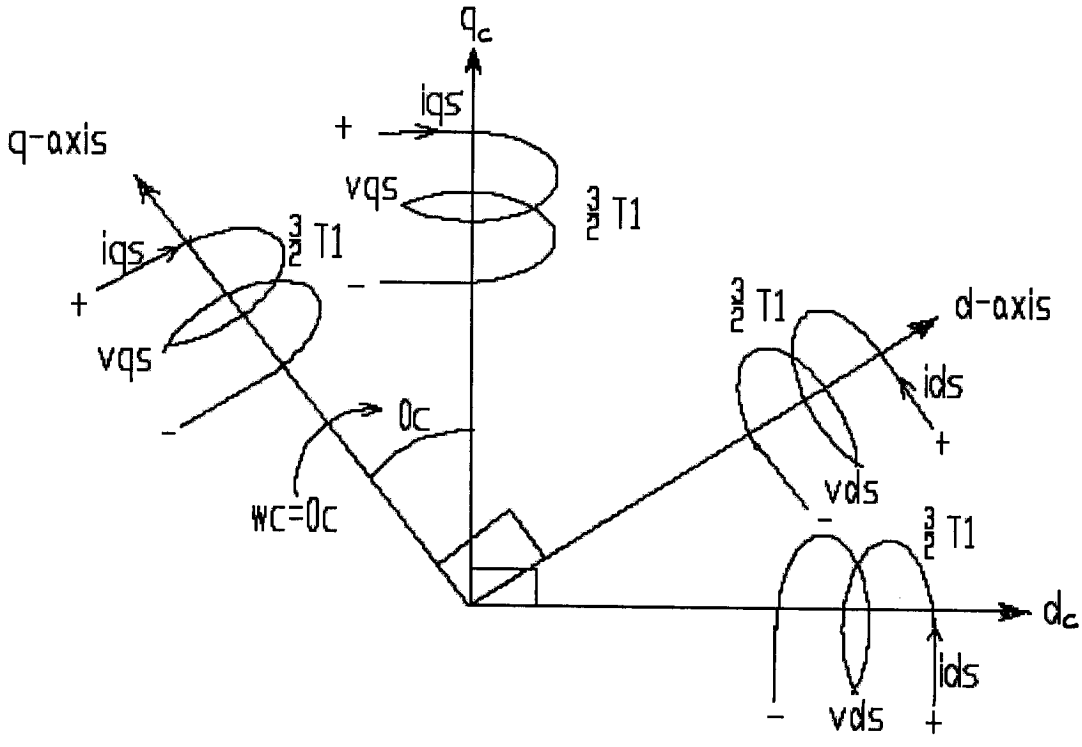

Figure 3.2: Stationary and arbitrary reference frames.

Assuming that the windings have equal number of turns on both of the reference frames, the arbitrary reference frame currents and voltages are resolved on the *d* and *q* axes to find the currents and voltages in the stationary reference frames. Various relationships and transformations are used to obtain the induction motor model in arbitrary reference frames (3.8) below [3,4,5].

$$\begin{bmatrix} v_{qs} \\ v_{ds} \\ v_{qr} \\ v_{dr} \end{bmatrix} = \begin{bmatrix} R_s + L_s p & \omega_c L_s & L_m p & \omega_c L_m \\ -\omega_c L_s & R_s + L_s p & -\omega_c L_m & L_m p \\ L_m p & (\omega_c - \omega_r) L_m & R_s + L_r p & (\omega_c - \omega_r) L_r \\ -(\omega_c - \omega_r) L_m & L_m p & -(\omega_c - \omega_r) L_r & R_s + L_r p \end{bmatrix} \begin{bmatrix} i_{qs} \\ i_{ds} \\ i_{qr} \\ i_{dr} \end{bmatrix} \quad (3.8)$$

where the speed of the arbitrary reference frame is

$$ó_c = \omega_c$$

and $\acute{o}_r = \omega_r$, ω_r is the rotor speed in electrical radian/sec.

Three particular cases of the generalized model of the induction motor in arbitrary reference frames are of general interest:

(i) Stator reference frames model;

(ii) Rotor reference frames model;

(iii) Synchronously rotating reference frames model.

3.2.1 **Stator Reference Frames Model**

It is usual to align the *q*-axis with the phase *a* winding; this implies that the *qd* axis are fixed to the stator. This model is also known as Stanley's model [5]. In this case, θ_c =0, and is substituted into (3.5) for the transformation from *abc* to *qdo.*

The speed of the reference frame is that of the stator, which is zero; hence

$$\omega_c=0$$

is substituted into equation (3.8).The resulting model is

$$\begin{bmatrix} v_{qs} \\ v_{ds} \\ v_{qr} \\ v_{dr} \end{bmatrix} = \begin{bmatrix} R_s + L_s p & 0 & L_m p & 0 \\ 0 & R_s + L_s p & 0 & L_m p \\ L_m p & -\omega_r L_m & R_r + L_s p & -\omega_r L_r \\ \omega_r L_m & L_m p & \omega_r L_r & R_r + L_s p \end{bmatrix} \begin{bmatrix} i_{qs} \\ i_{ds} \\ i_{qr} \\ i_{dr} \end{bmatrix} \tag{3.9}$$

With the applied phase voltages as follows:

$$v_{as} = \frac{240}{\sqrt{3}}.\sqrt{2}Sin\omega t = 196Sin\omega t \tag{3.10}$$

$$v_{bs} = 196Sin\left(\omega t - \frac{2\pi}{3}\right) \tag{3.11}$$

$$v_{cs} = 196Sin\left(\omega t + \frac{2\pi}{3}\right) \tag{3.12}$$

The q and d axes voltages are:

$$\begin{bmatrix} v_{qs} \\ v_{ds} \\ v_o \end{bmatrix} = \left[\frac{2}{3}\right] \begin{bmatrix} 1 & -\frac{1}{2} & -\frac{1}{2} \\ 0 & -\frac{\sqrt{3}}{2} & \frac{\sqrt{3}}{2} \\ \frac{1}{2} & \frac{1}{2} & \frac{1}{2} \end{bmatrix} \begin{bmatrix} v_{as} \\ v_{bs} \\ v_{cs} \end{bmatrix} \tag{3.13}$$

Hence,

$$v_{qs} = \frac{2}{3}\left[v_{as} - \frac{1}{2}(v_{bs} + v_{cs}) \right] \tag{3.14}$$

For a balanced three-phase input; $v_{as} + v_{bs} + v_{cs} = 0$

Substituting for v_{bs} and v_{cs} in terms of v_{as} yields

$$v_{qs} = v_{as} = 196 Sin\omega t = 196\angle 0 = 196 \text{ V} \tag{3.15}$$

Similarly,

$$v_{ds} = \frac{1}{\sqrt{3}}(v_{cs} - v_{bs}) = 196 Cos\omega t = 196\angle 90 = j196 \text{ V} \tag{3.16}$$

and $v_o = 0$. (3.17)

When the rotor is locked, ω_r=0 and for steady-state evaluation p=$j\omega_s$=j314.2 rad/s.

From (3.9) the system equations in steady-state are

$$\begin{bmatrix} 196 \\ j196 \\ 0 \\ 0 \end{bmatrix} = \begin{bmatrix} R_s + L_s p & 0 & L_m p & 0 \\ 0 & R_s + L_s p & 0 & L_m p \\ L_m p & -\omega_r L_m & R_r + L_s p & 0 \\ 0 & L_m p & 0 & R_r + L_s p \end{bmatrix} \begin{bmatrix} i_{qs} \\ i_{ds} \\ i_{qr} \\ i_{dr} \end{bmatrix} \tag{3.18}$$

Note that the rotor windings are short-circuited and hence rotor voltages are zero. The numerical values for the parameters and variables were substituted to solve for the currents. Running the stator.m file listed in Appendix A, Matlab return the following currents.

$$i_{qs} = 5.449 - j4.948 = 7.360\angle -42.24\,\text{A}$$

$$i_{ds} = -4.948 - j5.449 = 7.360\angle -132.24\,\text{A}$$

$$i_{qr} = -5.496 + j4.614 = 7.176\angle 139.98\ \text{A}$$

$$i_{dr} = 4.614 + j5.496 = 7.176\angle 49.98\ \text{A} \qquad (3.19)$$

and the phase currents are:

$$i_{as} = 7.36\angle 42.24\ A$$

$$i_{bs} = 7.36\angle -77.76\ A$$

$$i_{cs} = 7.36\angle 162.24\ A \qquad (3.20)$$

which can be rewritten as:

$$i_{as}=7.36\ \text{Sin}(\omega_s t+0.74)$$

$$i_{bs}=7.36\ \text{Sin}(\omega_s t-1.36)$$

$$i_{cs}=7.36\ \text{Sin}(\omega_s t+2.83) \qquad (3.21)$$

Using equations (3.21), a Matlab script in appendix D1was developed to plot the stator phase currents as shown in figure 3.3 below. The observed three-phase stator *abc* currents are balanced and have leading power factor angle of 42.24 °. The peak current value was 7.36 A and the corresponding rms of magnitude 5.20 A.

This model is used when stator variables are required to be actual, i.e. the same as in the actual machine stator, and rotor variables can be fictitious. This model allows elegant simulation of stator- controlled induction motor drives, such as phase controlled and inverter-controlled induction motor drives, because the input variables are well defined.

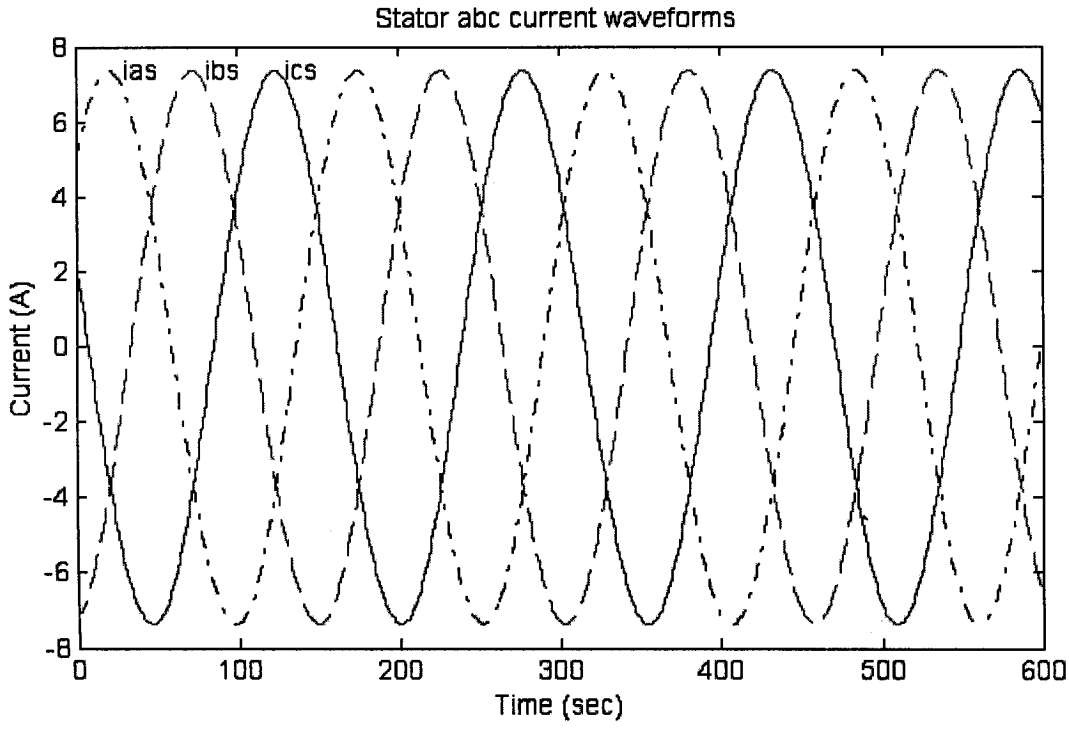

Figure 3.3: Stator *abc* currents waveforms derived from stator reference frame model.

3.2.2 **Rotor Reference Frames Model**

The speed of rotor reference frame is:

$$\omega_c = \omega_r \tag{3.22}$$

and the angular position is

$$\theta_c = \theta_r = \omega_{sl} t \tag{3.23}$$

Substituting equation (3.22) into the equation (3.8), the induction motor model in rotor reference frames was obtained. The equations are given by

$$\begin{bmatrix} v_{qs} \\ v_{ds} \\ v_{qr} \\ v_{dr} \end{bmatrix} = \begin{bmatrix} R_s + L_s p & \omega_r L_s & L_m p & \omega_r L_m \\ -\omega_r L_s & R_s + L_s p & -\omega_r L_m & L_m p \\ L_m p & 0 & R_r + L_r p & 0 \\ 0 & L_m p & 0 & R_r + L_r p \end{bmatrix} \begin{bmatrix} i_{qs} \\ i_{ds} \\ i_{qr} \\ i_{dr} \end{bmatrix} \tag{3.24}$$

The transformation from *abc* to *dqo* variables is obtained by substituting (3.23) into $[T_{abc}]$ defined in (3.5) and with applied phase voltages as in (3.10)-(3.12) gives

$$\begin{bmatrix} v_{qs} \\ v_{ds} \\ v_o \end{bmatrix} = [T_{abc}] \begin{bmatrix} v_{as} \\ v_{bs} \\ v_{cs} \end{bmatrix} = \begin{bmatrix} v_m \sin \omega_{sl} t \\ v_m \cos \omega_{sl} t \\ 0 \end{bmatrix} = \begin{bmatrix} 0 - jv_m \\ v_m + j0 \\ 0 \end{bmatrix} \tag{3.25}$$

The stator voltages appear at slip frequency in rotor reference frames; hence, the currents at slip frequency in steady state. Choosing an arbitrary rotor speed; 2880rpm (301.6 rad), slip speed ω_{sl} is 12.6 rad. By substituting $p=j\ \omega_{sl}=j12.6$ in the system equations, the following is obtained.

$$\begin{bmatrix} -jv_m \\ v_m \\ 0 \\ 0 \end{bmatrix} = \begin{bmatrix} R_s + j\omega_{sl}L_s & \omega_r L_s & j\omega_{sl}L_m & \omega_r L_m \\ -\omega_r L_s & R_s + j\omega_{sl}L_s & -\omega_r L_m & j\omega_{sl}L_m \\ j\omega_{sl}L_m & 0 & R_r + j\omega_{sl}L_r & 0 \\ 0 & j\omega_{sl}L_m & 0 & R_r + j\omega_{sl}L_r \end{bmatrix} \begin{bmatrix} i_{qs} \\ i_{ds} \\ i_{qr} \\ i_{dr} \end{bmatrix} \tag{3.26}$$

By substituting the appropriate parameters into (3.26) and upon running the Matlab script file in Appendix B the rotor reference currents are

$$\begin{bmatrix} i_{qs} \\ i_{ds} \\ i_{qr} \\ i_{dr} \end{bmatrix} = \begin{bmatrix} 0.861\angle -138.11 \\ 0.861\angle -48.11 \\ 0.603\angle 85.998 \\ 0.603\angle -4.002 \end{bmatrix} A \tag{3.27}$$

that can be rewritten in terms of the slip frequency as follows

$$\begin{bmatrix} i_{qs} \\ i_{ds} \\ i_{qr} \\ i_{dr} \end{bmatrix} = \begin{bmatrix} 0.861Sin(\omega_{sl}t - 0.84) \\ 0.861Cos(\omega_{sl}t - 0.84) \\ 0.603Sin(\omega_{sl}t + 1.50) \\ 0.603Cos(\omega_{sl}t + 1.50) \end{bmatrix} A \tag{3.28}$$

and $$\begin{bmatrix} i_{as} \\ i_{bs} \\ i_{cs} \end{bmatrix} = \begin{bmatrix} -0.5747 - 0.6407j \\ -0.2675 + 0.8181j \\ 0.8422 - 0.1773j \end{bmatrix} = \begin{bmatrix} 0.861\angle 131.8917 \\ 0.861\angle -108.1066 \\ 0.861\angle 11.8883 \end{bmatrix} A \tag{3.29}$$

Hence, the instantaneous *abc* currents are

$$i_{as} = 0.861\ Sin(\omega_{sl}t + 2.3)$$

$$i_{bs} = 0.861\ Sin(\omega_{sl}t - 1.89)$$

$$i_{cs} = 0.861\ Sin(\omega_{sl}t + 0.21) \tag{3.30}$$

The observed three-phase stator *abc* currents are balanced and have leading power factor angle of 48.11°. The peak current value was 0.861A and the corresponding rms value of 0.61A.

Rotor reference frames model is useful where the switching elements and power are controlled on the rotor side. Slip-power recovery is one example where this model will find use in the simulation of the motor-drive system.

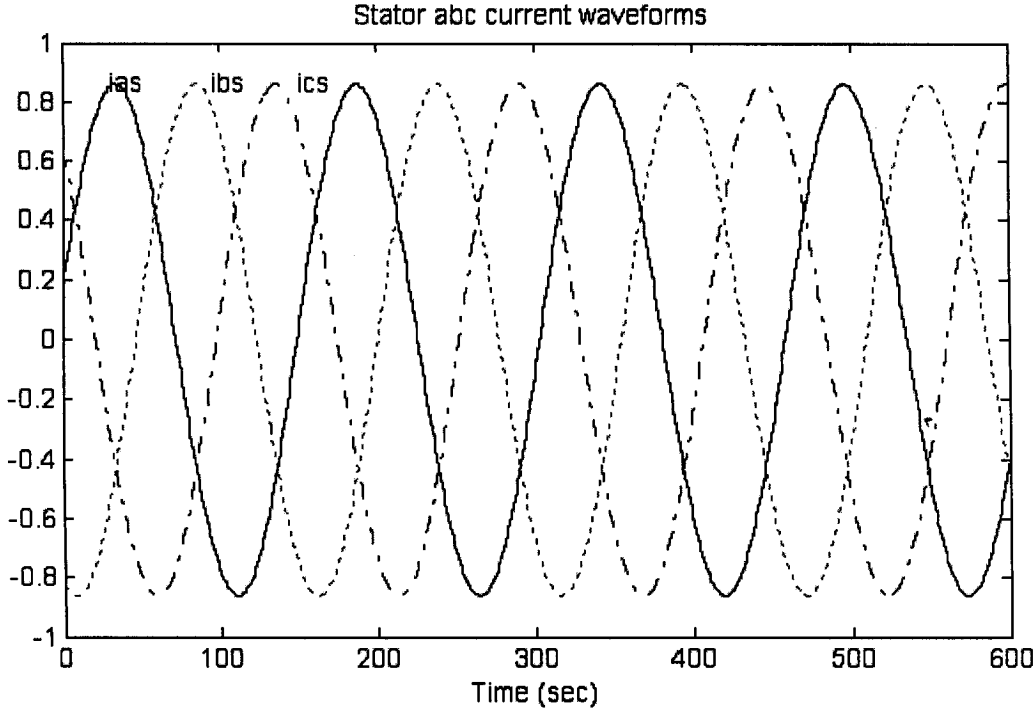

Figure 3.4: Stator *abc* currents waveforms derived from rotor reference frame model.

3.2.3 **Synchronously Rotating Reference Frame Model**

The speed of the reference frame is

$$\omega_c = \omega_s = \text{stator supply frequency (rad/s)} \tag{3.31}$$

and the instantaneous angular position is

$$\theta_c = \theta_s = \omega_s t \tag{3.32}$$

Transforming the applied voltages (equations (3.10)-(3.12)) to *dqo* variable in the synchronous reference frames, yields

$$\begin{bmatrix} v_{qs} \\ v_{ds} \\ v_o \end{bmatrix} = [T_{abc}] \begin{bmatrix} v_{as} \\ v_{bs} \\ v_{cs} \end{bmatrix} = \begin{bmatrix} 0 \\ v_m \\ 0 \end{bmatrix} \tag{3.33}$$

The *d* and *q* stator voltages are d.c quantities; hence, the response will be d.c quantities too, because the system is linear. Hence

$$pi_{qs} = pi_{ds} = pi_{qr} = pi_{dr} = 0. \tag{3.34}$$

Substituting (3.33)-(3.34) into the system equations (3.8) gives

$$\begin{bmatrix} 0 \\ v_m \\ 0 \\ 0 \end{bmatrix} = \begin{bmatrix} R_s & \omega_s L_s & 0 & \omega_s L_m \\ -\omega_s L_s & R_s & -\omega_s L_m & 0 \\ 0 & \omega_{sl} L_m & R_r & \omega_{sl} L_r \\ -\omega_{sl} L_m & 0 & -\omega_{sl} L_r & R_r \end{bmatrix} \begin{bmatrix} i_{qs} \\ i_{ds} \\ i_{qr} \\ i_{dr} \end{bmatrix} \tag{3.35}$$

where $\omega_{sl}=\omega_s-\omega_r=$*slip speed*

Taking an arbitrary rotor speed at 2880 *rpm* and angle at 90°, then $\omega_{sl}=12.6$ *rad/s*.
Replacing the numerical parameter values into equation (3.35) and running the Matlab script in Appendix C, the currents in synchronous reference frames are

$$\begin{bmatrix} i_{qs} \\ i_{ds} \\ i_{qr} \\ i_{dr} \end{bmatrix} = \begin{bmatrix} -0.5486 \\ 0.5315 \\ 0.0168 \\ -0.5349 \end{bmatrix} A \tag{3.36}$$

and the *abc* currents are

$$\begin{bmatrix} i_{as} \\ i_{bs} \\ i_{cs} \end{bmatrix} = \begin{bmatrix} 0.5315\ A \\ -0.7408\ A \\ 0.2094\ A \end{bmatrix} \tag{3.37}$$

Hence, the instantaneous *abc* currents are

$$i_{as} = 0.764\ Sin(\omega_s t + 0.8)$$

$$i_{bs} = 0.764\ Sin(\omega_s t + 2.894)$$

$$i_{cs} = 0.764\ Sin(\omega_s t - 1.294) \tag{3.38}$$

These *abc* stator currents were plotted as in fig.3.5 using Matlab script in Appendix D3.

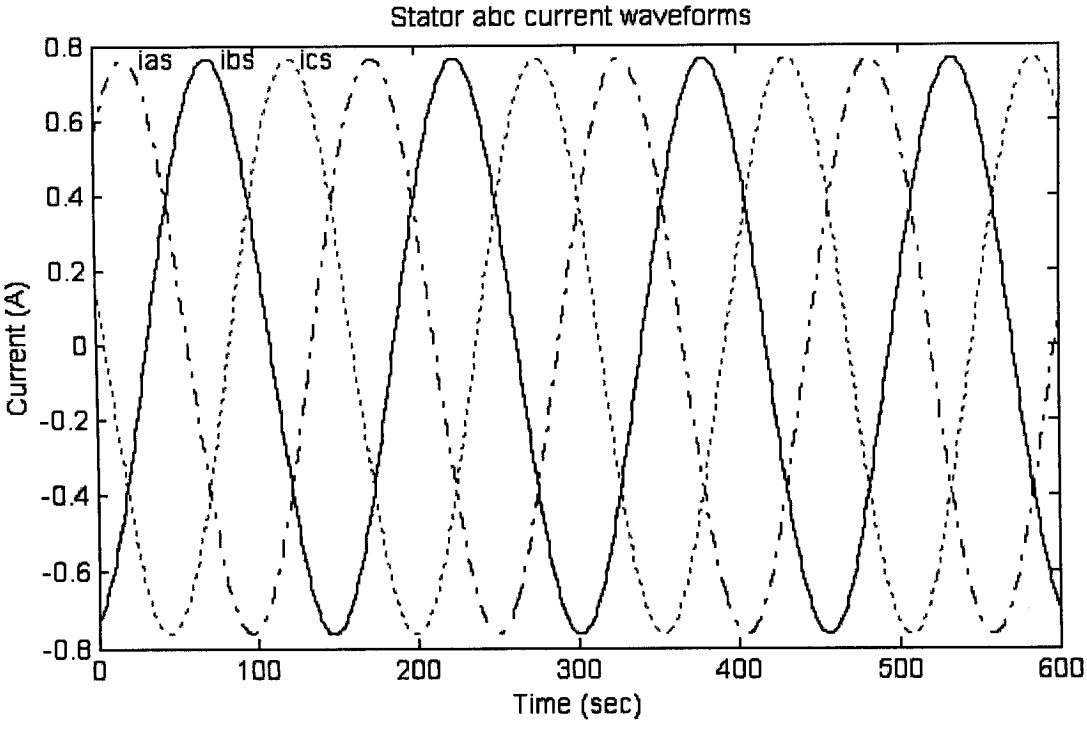

Figure 3.5: Stator *abc* currents waveforms derived from synchronous reference frames model at 2880 rpm

The observed three-phase stator *abc* currents are balanced and have leading power factor angle of 45.84 °. The peak current value is 0.764 A and the corresponding rms value of 0.540 A.

In order to observe the current behavior at different speeds, another arbitrary rotor speed of 2000 *rpm* and angle at 90° was taken. Then the new slip speed was 104.7rad/s and replacing slip speed 12.6 rad/s in Appendix C Matlab script the currents in synchronous reference frames are

$$\begin{bmatrix} i_{qs} \\ i_{ds} \\ i_{qr} \\ i_{dr} \end{bmatrix} = \begin{bmatrix} -1.6590 \\ 3.4674 \\ 1.2076 \\ -3.5240 \end{bmatrix} A \tag{3.39}$$

$$\begin{bmatrix} i_{qs} \\ i_{ds} \\ i_o \end{bmatrix} = \begin{bmatrix} -1.659 \\ 3.4674 \\ 0 \end{bmatrix} A \tag{3.40}$$

and the *abc* currents are

$$i_{abc} = \begin{bmatrix} 3.4674 \\ -3.1705 \\ -0.2970 \end{bmatrix} A \tag{3.41}$$

Hence, the instantaneous *abc* currents are

$$\begin{aligned} i_{as} &= 3.84Sin(\omega t - 0.44) \\ i_{bs} &= 3.84Sin(\omega t - 2.54) \\ i_{cs} &= 3.84Sin(\omega t - 1.65) \end{aligned} \tag{3.42}$$

The *abc* stator currents were plotted as in fig.3.5 using Matlab script in Appendix D4. At 2000 rpm the power factor angle is 25.2 ° lagging, and the peak current value and the corresponding rms value are 3.84 A and 2.72 A respectively. It was observed that with constant supply voltage the stator currents are very high at low speeds and reduces as the speed increases.

It was seen that the synchronous reference frames transform the sinusoidal input into d.c signals. Since the sinusoidal variables become d.c quantities, i.e. constants, and hence their derivatives, such as those of currents flux linkages in steady-state, are all zero. This help in visualizing the steady state much more than the models in other reference frames. This model is useful where the variables in steady-state need to d.c quantities. Some high performance control schemes use this model to estimate the control inputs; this led to a major breakthrough in induction-motor control, by decoupling the torque and flux channels for control in a similar manner to that for separately-excited d.c motor drives.

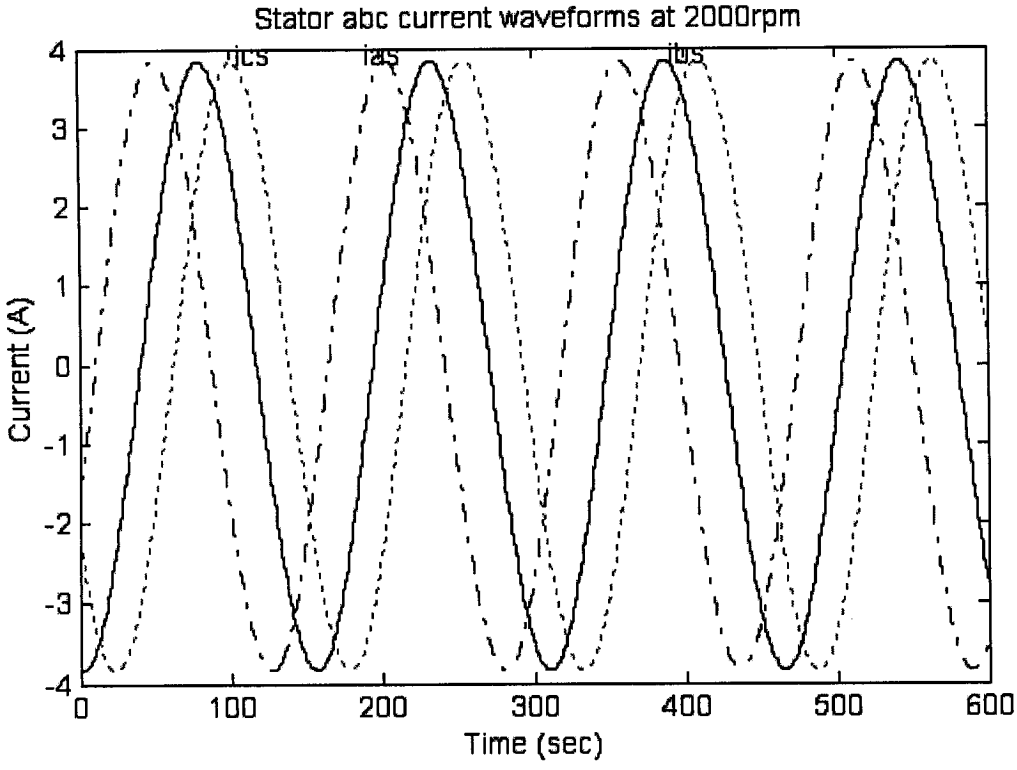

Figure 3.6: Stator *abc* currents waveforms derived from synchronous reference frame model at 2880 rpm

3.3 Induction Machine Simulation Using Simulink

In this section, state-variable models and simulation models have been adopted. A state-variable model is a differential equation model, but the equations are always written in a specific format. The state-variable model, or state-space model, is expressed as *n* first-order coupled differential equations. These equations preserve the system's input-output relationship (like that of a transfer function); in addition, an internal model of the system is given [6]. Some additional reasons for developing the state models are as follows:

1. Even if we do not implement the state-variable design (some may not be practical), we can produce a "best" system response.
2. State-variable models are generally required for digital simulation.
3. In state-variable design procedures, we feed back more information (internal variables) about the machine; hence, we can achieve a more complete control of the system than is possible with transfer function approach.

A simulation diagram or model is a certain type of either a block diagram or a flow graph that is constructed to have a specified transfer function or to model a specified set of differential equations. The simulation diagram is aptly named, since it is useful in constructing either digital or analogue computer simulations of a system.

3.3.1 **Stator Current Simulation.**

A d.c-step voltage is applied to one phase of the induction motor at standstill i.e. during the Locked-rotor test. Since we can access the neutral point of the stator windings star connection, we can excite only one phase and measure the phase current response. The equivalent per-phase circuit in this case is shown in figure 3.6. Since slip is unity, the rotor resistance will have maximum value in the sub-circuit. We neglected the core-loss resistance as its value acts like an open circuit for current through its branch.

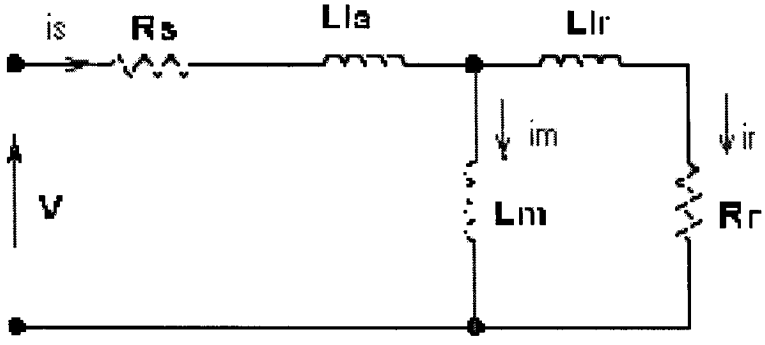

Figure 3.7: Equivalent per-phase circuit for d.c voltage applied in one motor phase

The current response to a step in phase voltage was determined by the circuit parameters. An analytical expression for this current was calculated as follows:

$$V_s = R_s i_s + L_{ls}\frac{di_s}{dt} + L_m\frac{di_n}{dt} \tag{3.43}$$

$$L_m\frac{di_m}{dt} = L_{lr}\frac{di_r}{dt} + R_r i_r \tag{3.44}$$

$$i_s = i_m + i_r \tag{3.45}$$

With (3.43) –(3.45) a second order differential equation for i_s can be derived:

$$(L_sL_r - L_{m\hat{}2})\frac{d\hat{}2i_s}{dt\hat{}2} + (R_sL_r - R_rL_s)\frac{di_s}{dt} + R_rR_s = R_rV_s \tag{3.46}$$

where $L_s = L_{ls} + L_m$ and $L_r = L_{lr} + L_m$

Equation (3.46) was further written as follows:

$$\frac{d\hat{}2i_s}{dt\hat{}2} = -\frac{(R_s + R_r)}{(L_rL_s - L_{m\hat{}2})}L_s\frac{di_s}{dt} - \frac{R_sR_r}{(L_rL_s - L_{m\hat{}2})}i_s + \frac{R_rV_s}{(L_rL_s - L_{m\hat{}2})} \tag{3.47}$$

and upon replacing actual parameter values yields

$$\frac{d\hat{}2i_s}{dt\hat{}2} = -369\frac{di_s}{dt} - 1400i_s + 221V_s \tag{3.48}$$

whence, the simulation model of figure 3.7 was constructed.

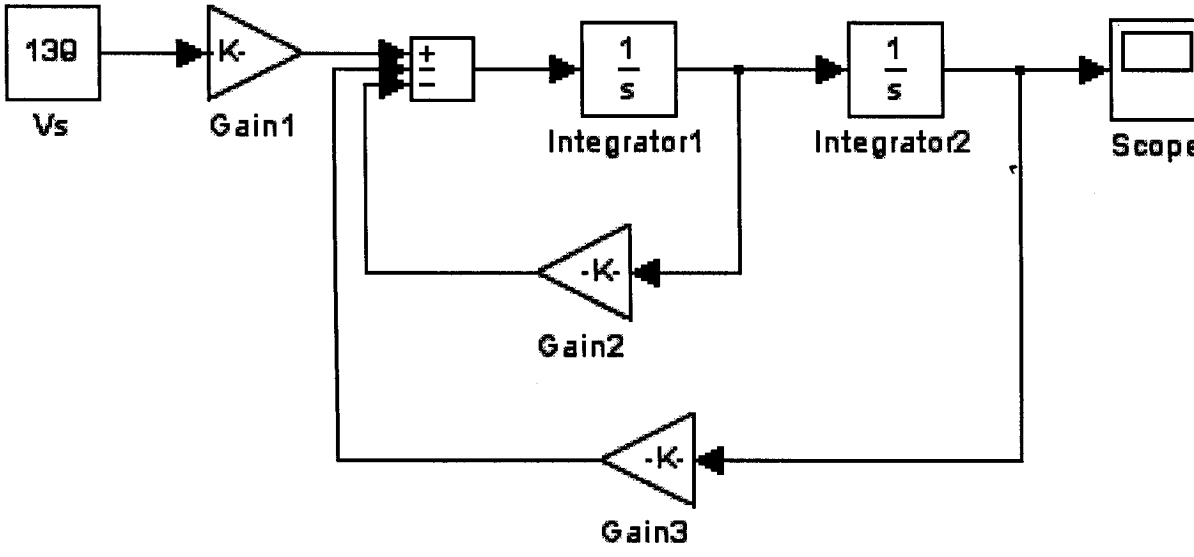

Figure 3.8: Simulation model for stator current

The simulation blocks of figure 3.8 found in the Simulink Block library are interpreted as follows:

- The input V_s (source) is a constant rms value of 139 V.
- Gain1 is constant set a value of 221.
- Gain2 is constant set a value of 369.
- Gain3 is constant set a value of 1400.

- Sink (scope) was for output observations

The stator current response to a step in phase voltage (139V) observed is shown in figure 3.9 and the steady-state solution of equation 3.48 is:

$$i_s(\infty) = \frac{V_s}{R_s}$$

.

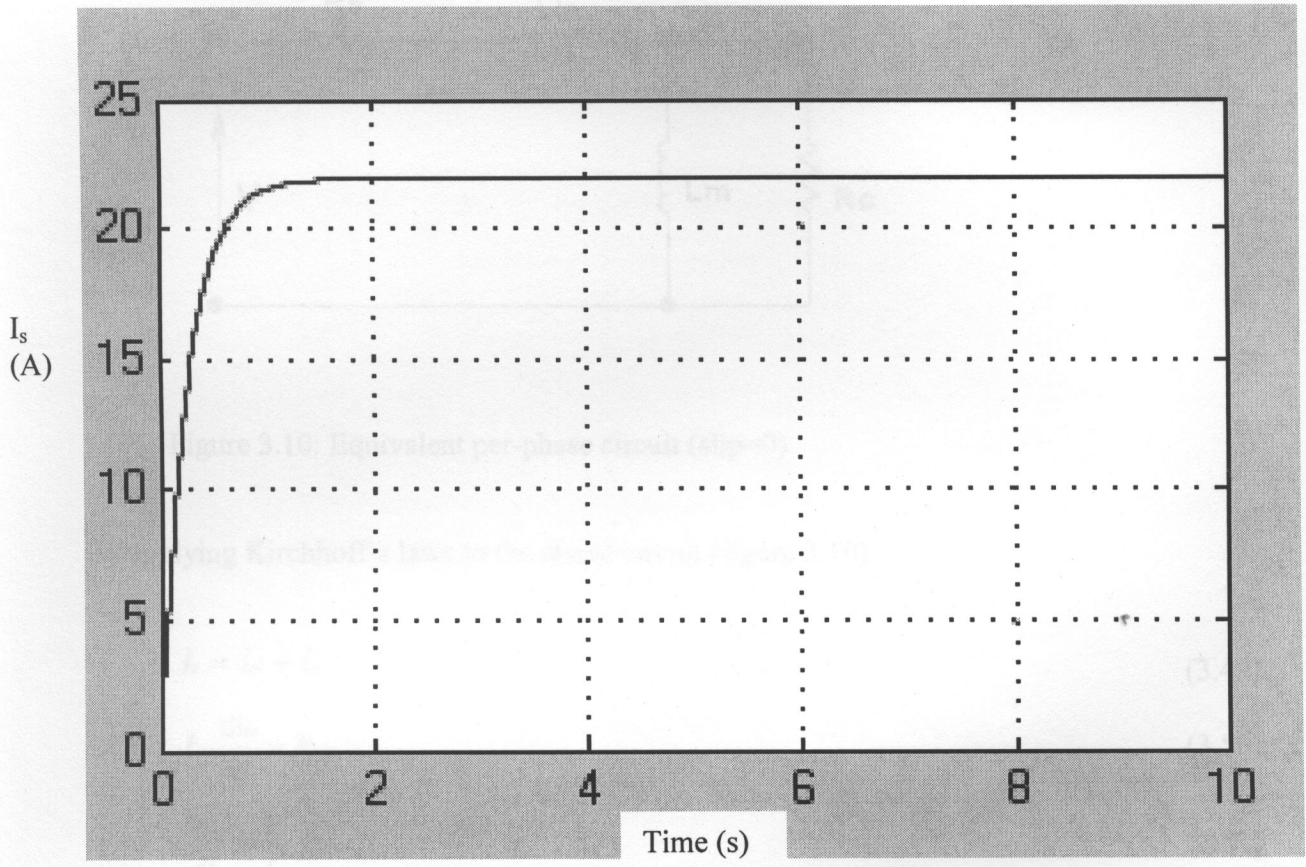

Figure 3.9: Stator current response to a step in phase voltage

3.3.2 Magnetizing Current Simulation

The magnetizing current simulation model was developed from the per-phase equivalent circuit at zero slip as shown below.

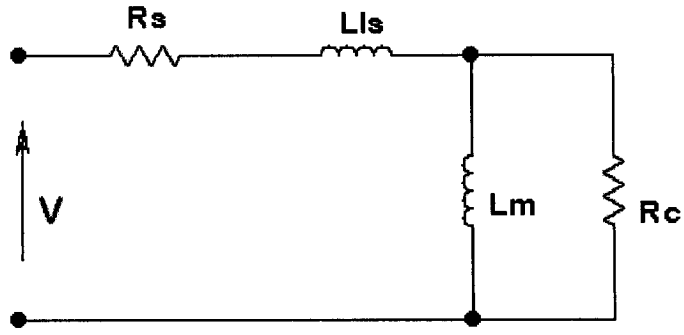

Figure 3.10: Equivalent per-phase circuit (slip=0)

By applying Kirchhoff's laws to the above circuit (figure 3.10),

$$i_s = i_m + i_c \tag{3.49}$$

$$L_m \frac{di_m}{dt} = R_c i_c \tag{3.50}$$

$$\frac{di_m}{dt} = \frac{R_c}{L_m}(i_s - i_m) \tag{3.51}$$

In terms the actual parameter values (3.51) can be written as

$$\frac{di_m}{dt} = 503(i_s - i_m) \tag{3.52}$$

whence the magnetizing current response simulation model in figure 3.11 was developed. Parameter Gain4 set to 503 and the rest of the constants and gains as for figure 3.8.

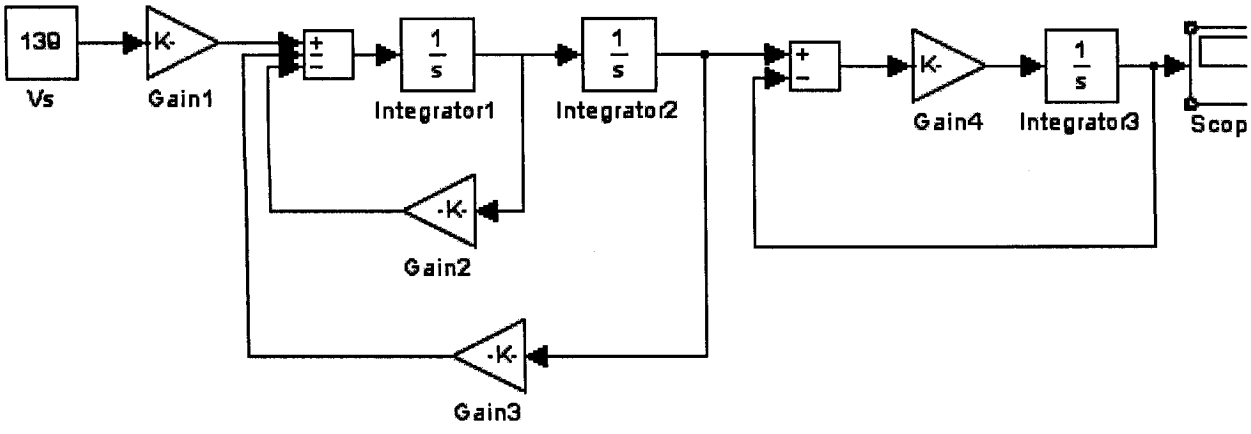

Figure 3.11: Simulation model for magnetising current response

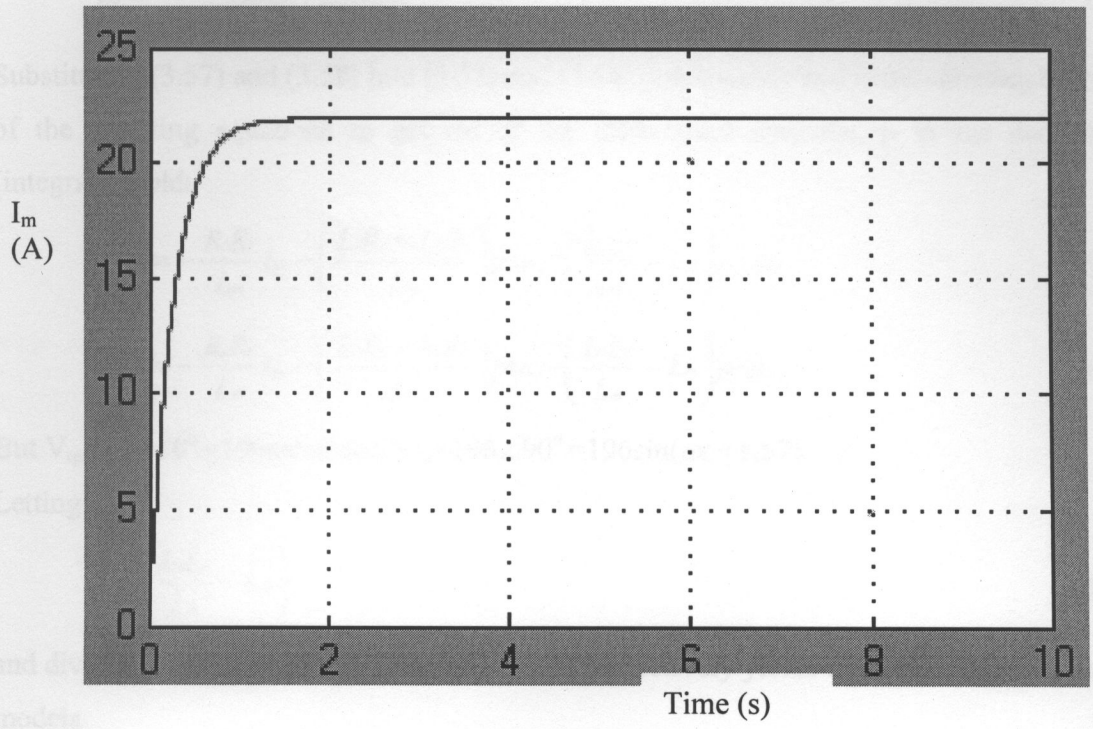

Figure 3.12: Magnetising current response

The core-loss resistance R_c was very large as it acts like an open circuit for the current through its branch, hence the magnetising current response was almost similar to the stator current response.

3.3.3 *q*- and *d*-axis Rotor Current Response

The *q*- and *d*-axis rotor current-time response state-variable models for the stator reference frames were developed from (3.18) written in the form:

$$V_{qs} = R_s i_{qs} + L_s p i_{qs} + L_m p i_{qr} \tag{3.53}$$

$$V_{ds} = R_s i_{ds} + L_s p i_{ds} + L_m p i_{dr} \tag{3.54}$$

$$V_{qr} = L_m p i_{qs} + R_r i_{qr} + L_r p i_{qr} \tag{3.55}$$

$$V_{dr} = L_m p i_{ds} + R_r i_{dr} + L_r p i_{dr} \tag{3.56}$$

But V_{qr} and V_{dr} are equal to zero, therefore (3.55) and (3.56) can be rewritten in term of i_{qs} and i_{ds} as

$$i_{qs} = -\frac{1}{L_m p}\left(R_r i_{qr} + L_r p i_{qr}\right) \tag{3.57}$$

$$i_{ds} = -\frac{1}{L_m p}\left(R_r i_{dr} + L_r p i_{dr}\right) \tag{3.58}$$

Substituting (3.57) and (3.58) into (3.53) and (3.54) respectively and differentiating both sides of the resulting equations to get rid of the differential operator, p in the denominator (integral), yields

$$pV_{qs} = -\frac{R_s R_r}{L_m} i_{qr} - \left(\frac{L_r R_s + L_s R_r}{L_m}\right) p i_{qr} - \left(\frac{L_s L_r}{L_m} - L_m\right) p\text{^}2 i_{qr} \tag{3.59}$$

$$pV_{ds} = -\frac{R_s R_r}{L_m} i_{dr} - \left(\frac{L_r R_s + L_s R_r}{L_m}\right) p i_{dr} - \left(\frac{L_s L_r}{L_m} - L_m\right) p\text{^}2 i_{dr} \tag{3.60}$$

But $V_{qs}=196\angle 0^{\circ}=196\sin\omega t$ and $V_{ds}=196\angle 90^{\circ}=196\sin(\omega t+1.57)$.

Letting

$$A = \left(\frac{L_s L_r}{L_m} - L_m\right) \tag{3.61}$$

and dividing both sides (3.59), (3.60) by (3.61) respectively yields the following state-variable models.

$$p\text{^}2 i_{qr} = -\left(\frac{L_r R_s + L_s R_r}{A L_m}\right) p i_{qr} - \frac{R_s R_r}{A L_m} i_{qr} - \frac{p V_{qs}}{A} \tag{3.62}$$

$$p\text{^}2 i_{dr} = -\left(\frac{L_r R_s + L_s R_r}{A L_m}\right) p i_{dr} - \frac{R_s R_r}{A L_m} i_{dr} - \frac{p V_{ds}}{A} \tag{3.63}$$

Substituting the actual parameter values of motor give

$$p\text{^}2 i_{qr} = -369\, p i_{qr} - 1400 i_{qr} + 3459 Sin(\omega t + 1.57) \tag{3.64}$$

and

$$p\text{^}2 i_{dr} = -369\, p i_{dr} - 1400 i_{dr} + 3459 Sin\,\omega t \tag{3.65}$$

Using equation (3.64) and (3.65), simulations diagram of figure 3.13 and 3.15 were constructed respectively. By using the similar approach, however, the simulation for *q*- and *d*-axis rotor current response in rotor and synchronously rotating reference frames were not achievable. This was because of non-linearity of the final equations obtained.

The simulation blocks of figure 3.13 found in the Simulink Block library are interpreted as follows:

-The input (source) is a sinewave with the following block parameters

Amplitude: 3459

Frequency (rad/s): 6.284

Phase (rad): 0

Sample time (s): 0.02

-Slider Gain1 set at constant value of 369.

-Slider Gain2 set at constant value of 1400.

-Sink (scope) was for results observations.

The simulation blocks for figure 3.15 are similar to ones above except for the phase that was set at 1.57 rad.

Simulation results of the two are shown in figure 3.14 and 3.16 below. Both the *q*-axis rotor current and *d*-axis rotor current are of rms magnitude of 0.884 A and 90° out of phase.

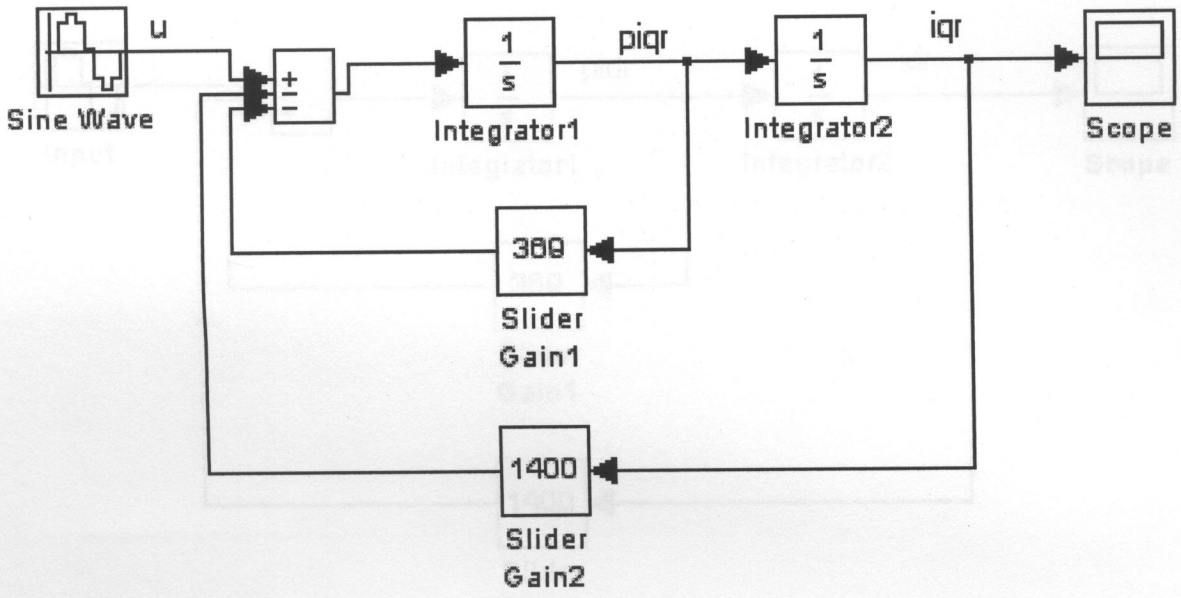

Figure 3.13: Simulation model for q-axis rotor current response

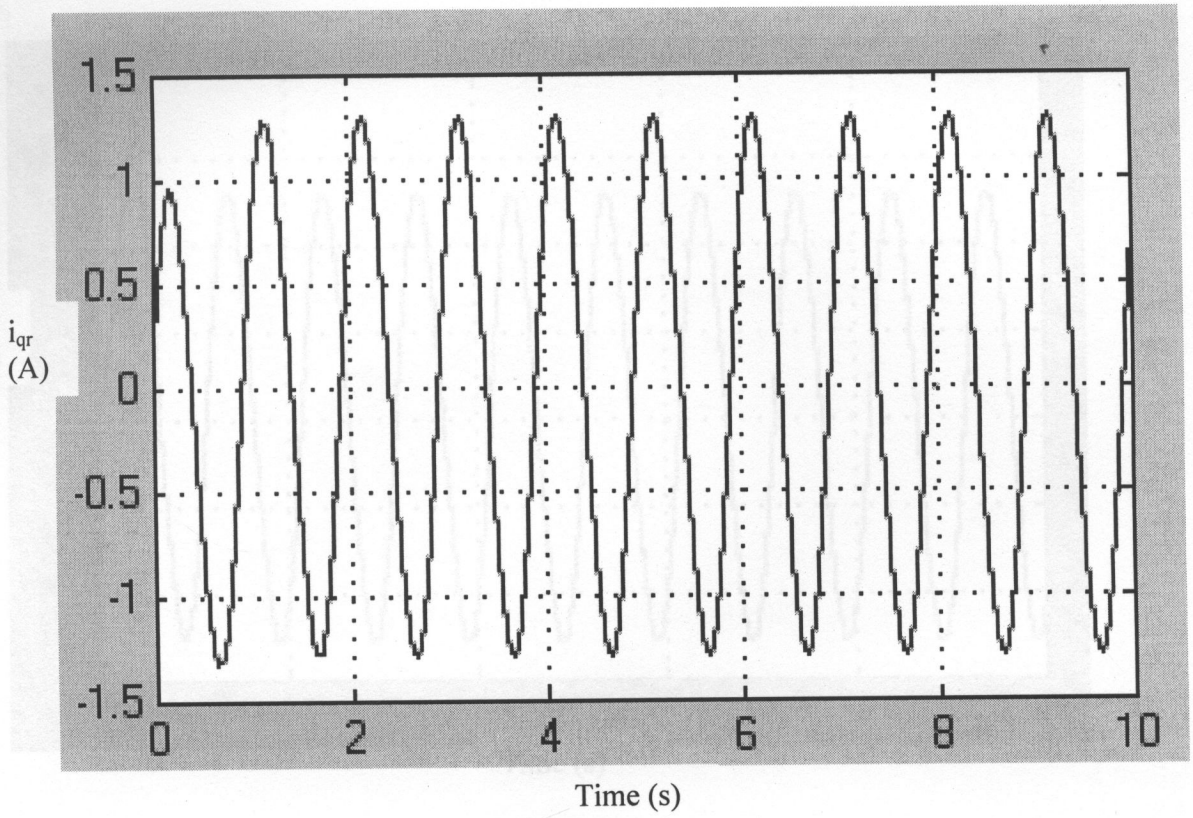

Figure 3.14: q-axis rotor current response

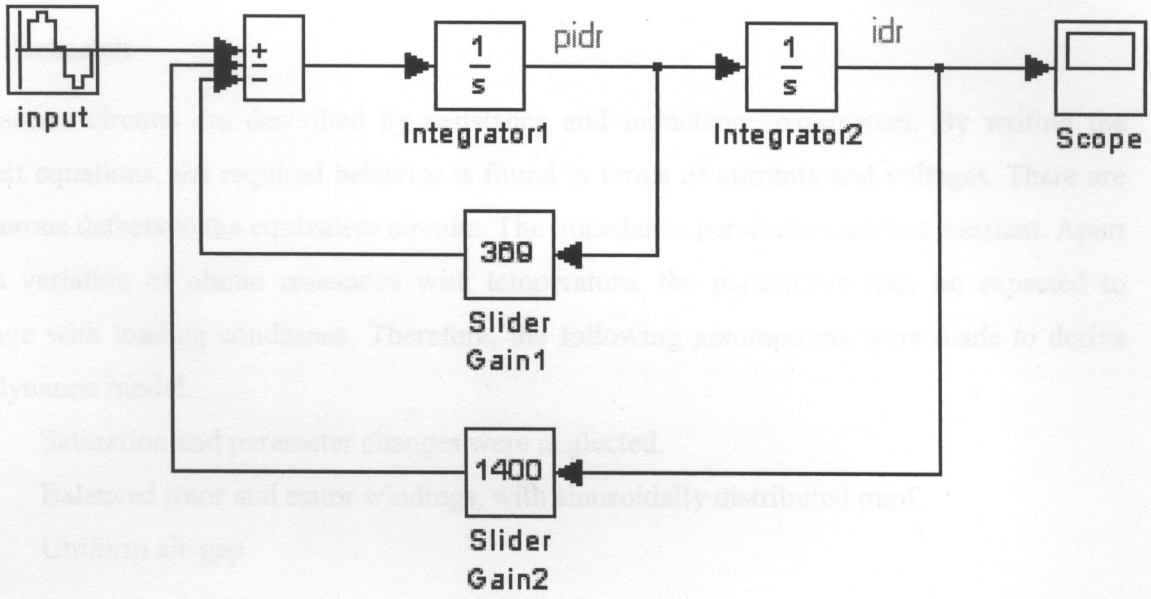

Figure 3.15: Simulation model for *d*-axis rotor current response

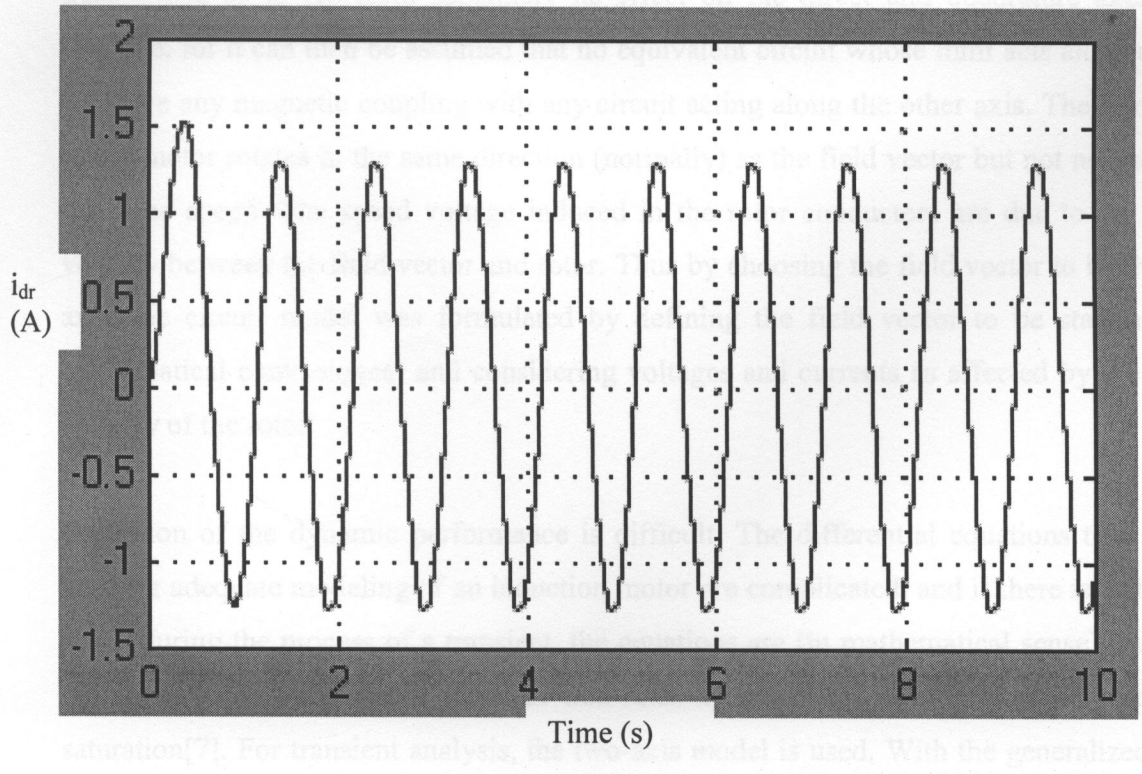

Figure 3.16: *d*-axis rotor current response

CHAPTER FOUR

4.0 DISCUSSIONS AND CONCLUSION

4.1 Discussion

All active circuits are described by resistance and inductance parameters. By writing the circuit equations, the required behavior is found in terms of currents and voltages. There are numerous defects in the equivalent circuits. The impedance parameters are not constant. Apart from variation of ohmic resistance with temperature, the parameters may be expected to change with loading conditions. Therefore, the following assumptions were made to derive the dynamic model.

i. Saturation and parameter changes were neglected.
ii. Balanced rotor and stator windings, with sinusoidally distributed mmf.
iii. Uniform air-gap

As any given circuit a machine may be magnetically coupled with any other, the circuit equations are complicated. Substantial simplification is achieved if each circuit is so transformed as to represent separately its effect on the direct and quadrature axes of the machine, for it can then be assumed that no equivalent circuit whose mmf acts along one axis can have any magnetic coupling with any circuit acting along the other axis. The rotor of the actual motor rotates in the same direction (normally) as the field vector but not necessarily at the same speed. The speed voltage induced in the rotor conductors are due to the relative velocity between the field vector and rotor. Thus by choosing the field vector to be the direct axis, the circuit model was formulated by defining the field vector to be stationary (for mathematical convenience) and considering voltages and currents as affected by the relative velocity of the rotor.

Prediction of the dynamic performance is difficult. The differential equations that must be used for adequate modeling of an induction motor are complicated, and if there is a change of speed during the process of a transient, the equations are (in mathematical sense) non-linear, quite apart from inevitable physical non-linearity resulting from deep- bar effects and saturation[7]. For transient analysis, the two-axis model is used. With the generalized model, the two-axis transient equivalent voltages for the case considered are imposed and the equations solved at any arbitrary speed. In the analysis presented in this report the rotor

circuits are short-circuited and have no external applied voltage so that $V_{qr}=V_{dr}=0$. The validity of the method was shown by presuming steady-state conditions with constant slip *s*. Then p was replaced by $j\omega_s$, $j\omega_{sl}$ and zero for the stator, rotor and synchronous rotating reference frames model respectively. The rotor and synchronously rotating reference frames models gave nearly the same current response magnitude at same speeds. The small differences arise from the simplification involved in each particular model.

The processes, was brief, is to transform a winding and its voltage and current into an equivalent coil on the *q*- and *d*- axis with the polyphase quantities thus converted into their axis equivalents; to set up the circuit equations for such circuit; impose the operating conditions; solve the equations; and finally to convert the solution back into terms of the currents and voltages of the actual machine windings.

4.2 Conclusion

In order to interpret the physical phenomena involved in the operation the motor, equations are set-up in which the axes are fixed with respect to the machine structure and by operating on these equations with transformation of variables. This provide (1) a second point of view, and thus a more complete understanding of the characteristics of the induction motor, and (2) a set of equations that relate the circuit model to the physical machine parameters.

To evaluate system performance it is necessary to have a quantitative model of each subsystem in the form of a set of equations or a simulation. The subsystem models are then interconnected with due regard to their individual constraints. The model of an induction motor can take many forms from simple elementary description in terms of current sheets to sophisticated equations in terms of voltage, current, speed and electrical parameters. Much depends on the use to which the model is to be put.

When the rotor is stationary (stator reference frames model), the induced voltage is of the same frequency as the supply, and the circulating current is quite large. Under running conditions, however, the frequency of the induced voltage in the rotor is quite low, and the current in the rotor is relatively small. In other words, the rotor currents become smaller as the rotor speed accelerates. Physical analysis of these observable features is given in section 3.2.1-3.2.3, followed by mathematical analyses based on the basic machine model.

An ever-present difficulty is magnetic saturation, which produces physical effects that are not readily made analytic in the mathematic model. In spite of these drawbacks, the generalized two- axis dynamic circuits theory has been found very powerful in the analysis of the motor. The more comprehensive the study, the more complex must be the model.

4.3 Recommendations

Initially, the performance features of the induction motor were voltage, current, speed, torque and power. The power and torque performance features were not done because of much time spent on the current, voltage and speed characteristic performances. In this regard, I wish to suggest that this project be considered for continuing project in future so that, with the work done so far, the torque and power performance features can be concentrated on.

REFERENCES

1. Fitzgerald, A.E, Kingsley, C, and Umans, S.D, "*Electrical Machinery*", fourth edition, McGraw-Hill, Inc, USA, 1983, pp 409-435.
2. Siskind, C.S, "*Electrical Machines*", second edition, McGraw-Hill, Inc, USA, 1959, pp 346-396.
3. Fitzgerald, A.E, and Kingsley, C, "*Electrical Machinery*", second edition, McGraw-Hill, Inc, New York, USA, 1961, pp 285-325.
4. George J.T, and Milton L.W, "*Electrical Machines*": *Dynamic and Steady state*, John Wiley and Sons, Inc, New York, 1966, pp 165-208.
5. Krishnan, R. "*Electric Motor Drives*": *Modeling, Control and Analysis*, Prentice-Hall, India, 2003. pp 174-255
6. Charles, L.P, and Royce, D.H, "*Feedback Control Systems*", fourth edition, Prentice-Hall, Inc, USA, 2000
7. Say, M.G, " *Alternating Current Machines*", fifth edition, longman, Singapore, 1983.
8. Matlab and Simulink help desk or http://www.mathworks.com

APPENDICES

Appendix A

```
>> % Stator.m script file

>> z(1,1)=6.34+314.2*1.152j; % poke in the non-zero values as needed
>> z(1,3)=314.2*1.124j;
>> z(2,2)=6.34+314.2*1.152j;
>> z(2,4)=314.2*1.124j;
>> z(3,1)=314.2*1.124j;
>> z(3,3)=14.07+314.2*1.152j;
>> z(4,2)=314.2*1.124j;
>> z(4,4)=14.07+314.2*1.152j;
>>
>> v=[196 196j 0 0]';  %voltage vector
>> i=z\v                % complex current vector solution i.e [ iqs, ids, iqr, idr]'

i =

  5.4491 - 4.9480i
 -4.9480 - 5.4491i
 -5.4960 + 4.6141i
  4.6141 + 5.4960i

>> imag=abs(i)      % magnitude current solution i.e [ iqs, ids, iqr, idr]'

imag =

   7.3604
   7.3604
   7.1761
   7.1761

>> iphase=angle(i)*180/pi  % solution phases in degree

iphase =

  -42.2407
 -132.2407
  139.9853
   49.9853

>> T(1,1)=1;  %transformation from two-phase to three-phase
>> T(1,3)=1;
>> T(2,1)=-1/2;
>> T(2,2)=-sqrt(3)/2;
>> T(2,3)=1;
>> T(3,1)=-1/2;
>> T(3,2)=sqrt(3)/2;
```

```
>> T(3,3)=1;
>> b=[5.4491-4.948j -4.948-5.4491j 0]';
>> a=T*b      % abc phase currents i.e [i_as, i_bs, i_cs]'

a =

  5.4491 + 4.9480i
  1.5605 - 7.1931i
 -7.0096 + 2.2451i

>> amag=abs(a)   % abc phase current magnitudes i.e [i_as, i_bs, i_cs]'

amag =

   7.3604
   7.3604
   7.3604

>> aphase=angle(a)*180/pi    % solution phases in degree

aphase =

  42.2407
 -77.7593
 162.2407
```

Appendix B

```
% Rotor .m Script file
>> z(1,1)=6.34+12.6*1.152j; % form an impedance matrix
>> z(1,2)=301.6*1.152;
>> z(1,3)=12.6*1.124j;
>> z(1,4)=301.6*1.124;
>> z(2,1)=-301.6*1.152;
>> z(2,2)=6.34+12.6*1.152j;
>> z(2,3)=-301.6*1.124;
>> z(2,4)=12.6*1.124j;
>> z(3,1)=12.6*1.124j;
>> z(3,3)=14.07+12.6*1.152j;
>> z(4,2)=12.6*1.124j;
>> z(4,4)=14.07+12.6*1.152j;
>> v=[-196j 196 0 0]';
>> idq=z\v                %rotor reference frame currents.

idq =

 -0.6407 - 0.5747i
 -0.5747 + 0.6407i
  0.0421 + 0.6015i
  0.6015 - 0.0421i

>> idqmag=abs(idq)

idqmag =

   0.8607
   0.8607
   0.6030
   0.6030

>> idqphase=angle(idq)

idqphase =

  -2.4105
   2.3019
   1.5010
  -0.0698

>> idqphase=angle(idq)*180/pi

idqphase =

 -138.1095
  131.8905
```

```
  85.9983
  -4.0017

>> T(1,2)=1;        % Transformation matrix with wt (θr) at pi/2
>> T(1,3)=1;
>> T(2,1)=sqrt(3)/2;
>> T(2,2)=-1/2;
>> T(2,3)=1;
>> T(3,1)=-sqrt(3)/2;
>> T(3,2)=-1/2;
>> T(3,3)=1;
>> A=[idq(1,1) idq(2,1) 0]'

A =

  -0.6407 + 0.5747i
  -0.5747 - 0.6407i
        0

>> iabc=T*A            % Stator abc currents at pi/2

iabc =

  -0.5747 - 0.6407i
  -0.2675 + 0.8181i
   0.8422 - 0.1773i
```

Appendix C

```
>> % Synchronous.m Script file.

>> z(1,1)=6.34;
>> z(1,2)=314.2*1.152;
>> z(1,4)=314.2*1.124;
>> z(2,1)=-314.2*1.152;
>> z(2,2)=6.34;
>> z(2,3)=-314.2*1.124;
>> z(3,2)=12.6*1.124;
>> z(3,3)=14.07;
>> z(3,4)=12.6*1.152;
>> z(4,1)=-12.6*1.124;
>> z(4,3)=-12.6*1.152;
>> z(4,4)=14.07;
>> v=[0 196 0 0]';
>> iqdo=z\v
iqdo =

  -0.5486
   0.5315
   0.0168
  -0.5349
>> T(1,2)=1;
>> T(1,3)=1;
>> T(2,1)=sqrt(3)/2;
>> T(2,2)=-1/2;
>> T(2,3)=1;
>> T(3,1)=-sqrt(3)/2;
>> T(3,2)=-1/2;
>> T(3,3)=1;
>> i=[iqdo(1,1) iqdo(2,1) 0]'
i =

  -0.5486
   0.5315
        0
>> iabc=T*i

iabc =

   0.5315
  -0.7408
   0.2094

>> ias=0.764sin(ωst+0.8)
>> ibs=0.764sin(ωst+2.894)
>> ics=0.764sin(ωst-1.294)
```

Appendix D1

```
>> % Script for the stator abc current waveforms
>> t=[0:600];
>> w=314.2;
>> ias=7.36*sin(w*t+0.74);
>> ibs=7.36*sin(w*t-1.36);
>> ics=7.36*sin(w*t+2.83);
>> plot(t,ias,'-.',t,ibs,'--',t,ics)
>> title('Stator abc current waveforms')
>> xlabel('Time (sec)')
>> ylabel('Current (A)')
>> text(30,7.36,'ias')
>> text(80,7.36,'ibs')
>> text(130,7.36,'ics')
```

Appendix D2

```
>> %Script for plotting the stator abc currents
>> %derived from rotor reference frame model
>> t=[0:600];
>> w=314.2;
>> ias=0.861*sin(w*t+2.3);
>> ibs=0.861*sin(w*t-1.89);
>> ics=0.861*sin(w*t+0.21);
>> plot(t,ias,'-.',t,ibs,':',t,ics,'k')
>> xlabel('Time (sec)')
>> title('Stator abc current waveforms')
>> text(30,0.86,'ias')
>> text(95,0.86,'ibs')
>> text(150,0.86,'ics')
```

Appendix D3

```
>> %Script for plotting the stator abc currents derived from synchronous
>> % reference frame model with rotor speed at 2880rpm (301.6rad/s)
>> t=[0:600];
>> w=314.2;
>> ias=0.764*sin(w*t+0.8);
>> ibs=0.764*sin(w*t+2.894);
>> ics=0.764*sin(w*t-1.294);
>> plot(t,ias,'-.',t,ibs,':',t,ics,'k')
>> xlabel('Time (sec)')
>>  ylabel('Current (A)')
>> title('Stator abc current waveforms')
>> text(30,0.76,'ias')
>> text(80,0.76,'ibs')
>> text(130,0.76,'ics')
```

Appendix D4

```
>> %Script for plotting the stator abc currents derived from synchronous
>> % reference frame model with rotor speed at 2000rpm (209raad/s)
>> t=[0:600];
>> w=314.2;
>> ias=3.84*sin(w*t-0.44);
>> ibs=3.84*sin(w*t-2.54);
>> ics=3.84*sin(w*t-1.65);
>> plot(t,ias,'-.',t,ibs,':',t,ics,'k')
>> title('Stator abc current waveforms at 2000rpm')
>> xlabel('Time (sec)')
>> ylabel('Current (A)')
>> text(190,3.9,'ias')
>> text(390,3.9,'ibs')
>> text(105,3.9,'ics')
```